

Article

Metabolome and Transcriptome Analyses Reveal the Differences in the Molecular Mechanisms of Oat Leaves Responding to Salt and Alkali Stress Conditions

Jianhui Bai ¹, Peina Lu ², Feng Li ³, Lijun Li ^{1,*} and Qiang Yin ^{3,†}

¹ Agricultural College, Inner Mongolia Agricultural University, Hohhot 010018, China; bzmayyb@163.com

² State Key Laboratory of Aridland Crop Science, Gansu Agricultural University, Lanzhou 730070, China; peina112@163.com

³ Institute of Grassland Research of Chinese Academy of Agricultural Sciences, Hohhot 010010, China; feng2021a2@163.com (F.L.); yinqiangyq12@163.com (Q.Y.)

* Correspondence: junli6@163.com

† These authors contributed equally to this work.

Abstract: Plant growth and production are more severely inhibited by alkalinity than by salinity. However, the metabolites responsible for the reduced growth caused by alkalinity are largely unknown. Here, the Illumina RNA-Seq analysis and targeted metabolome were used to identify the differentially expressed genes and metabolites responding to salt and alkali stresses. The expression levels of eight genes related to photosynthesis and some genes related to chlorophyll synthesis decreased under alkali stress, whereas no changes were detected under salt stress, which may explain the observed lower level of photosynthetic rate in alkalinity than in salinity. Under alkali stress, significant decreases in the relative abundances of cis-cinnamic acid and scopolin were observed, which correlated with the high levels of reactive oxygen species (ROS). The levels of protocatechuic acids decreased, correlating with the observed decrease in the chlorophyll content. Alkalinity markedly increased the production of o-coumaric acid, which contributes to growth inhibition. No significant changes in cis-cinnamic acid, scopolin, and o-coumaric acid were detected in salinity, which may be the reason for the stronger growth inhibition due to alkali stress than salt stress. The accumulation of citric acid, serotonin, pyroglutamic acid, L-citrulline, ferulic acid, and caffeic acid was detected under salt and alkali stress conditions, indicating high free radical scavenging capacity. The enhancement of mevalonic acid and salicylic acid levels was detected under alkali stress, which could have facilitated chlorophyll accumulation. Salt and alkali stress conditions also led to the accumulation of cyclic AMP related to inorganic ion regulation and betaine-related osmoregulation. Benzamide, phenethylamine, N-feruloyltyramine, chrysoeriol 6-C-hexoside, 1,3-di-p-coumaroyl glycerol, cordycepin, and 1-o-p-coumaroylglycerol were identified to be accumulated in response to alkali stress.

Keywords: alkali stress; salt stress; metabolome; transcriptome; oat



Citation: Bai, J.; Lu, P.; Li, F.; Li, L.; Yin, Q. Metabolome and Transcriptome Analyses Reveal the Differences in the Molecular Mechanisms of Oat Leaves Responding to Salt and Alkali Stress Conditions. *Agronomy* **2023**, *13*, 1441. <https://doi.org/10.3390/agronomy13061441>

Academic Editor: Cinzia Margherita Berteà

Received: 15 April 2023

Revised: 13 May 2023

Accepted: 18 May 2023

Published: 23 May 2023



Copyright: © 2023 by the authors. Licensee MDPI, Basel, Switzerland. This article is an open access article distributed under the terms and conditions of the Creative Commons Attribution (CC BY) license (<https://creativecommons.org/licenses/by/4.0/>).

1. Introduction

Soil salinization adversely affects crop yield and quality [1–3]. Salinized soil occupies more than 800 million hectares on earth. Almost one-third of the arable farmland in China is affected by salt stress [4]. It has been estimated that 50% of cultivated land may be affected by salinity by 2050 [5].

Salinized soil includes soil with neutral salts (Na_2SO_4 and NaCl) and alkaline salts (Na_2CO_3 and NaHCO_3). Neutral salts exert osmotic and ionic stress conditions. Alkaline salts not only exert these two stress conditions but also exert high pH stress. Therefore, alkalinity has more destructive effects on plants than salinity [6]. For example, a lower oat yield was observed with 75 mmol.L^{-1} alkalinity treatment as compared to 150 mmol.L^{-1}

salinity treatment [7]. However, to date, more attention has been devoted to neutral salts. Accordingly, several strategies to increase neutral salt stress tolerance in plants have been identified, including ion compartmentalization, hormonal regulation, osmotic regulation, and up-regulation of proteins and antioxidant enzymes such as monodehydroascorbate reductase, which can promote the elimination of reactive oxygen species (ROS) [8–11]. However, few studies have investigated alkali stress despite alkali stress being of increasing concern due to its threat to crop production.

As end products of biological processes, metabolites are likely related to phenotypes. Metabolites participate in many plant biological processes, such as cell signalling, cell formation and integrity, energy allocation and storage, and growth [12–14]. Metabolites are closely involved in the improvement of tolerance to abiotic stress via modification of physiological pathways. The mechanisms by which metabolites participate in the response to salt stress have been reported. For example, increasing levels of amino acids such as isoleucine, lysine, and valine have been reported in the roots of common bean (susceptible genotype) under salt stress [5], whereas altered levels of organic acids (such as gluconic acid, oxaloacetic acid, etc.), polyhydric alcohols (ribitol, inositol, etc.), phenolic acids (cinnamic acid, ferulic acid), and flavonoids (protocatechuic acid) have been observed in sesame and *Arabidopsis thaliana* under salinity [4,15,16]. Moreover, an improvement in flavonoid levels has been reported in *Sorghum bicolor* under salt–alkali stress [17], whereas other studies have reported that altered levels of amino acids and organic acids contribute to improved alkali tolerance in alfalfa and cotton [18,19].

In our previous study, we found that the effects of salt and alkali stress conditions on oats differed. Specifically, alkalinity led to the presence of yellow leaves, with limited chlorophyll accumulation, whereas salinity caused many dry leaves, with a disrupted water balance [7]. Moreover, lower photosynthetic rates and oat yields have been observed under alkali stress as compared to salt stress [20]. It has been reported that salt, alkali, saline–alkali mixed stress all decreased photosynthetic indices of apple *Malus Halliana*, and the extent of reductions in photosynthetic rate (P_n) and intercellular CO_2 concentration (C_i) under alkali stress were all significantly greater than those under salt and saline–alkali mixed stresses [21].

On the other hand, metabolites affect crop yields. Research has demonstrated that several metabolites (such as glycerol, valine, etc.) are negatively correlated with grain yield, whereas other metabolites such as succinate and fumarate are positively correlated with grain yield [22]. Therefore, it is essential to explore the differences in metabolic pathways in response to salt and alkali stress conditions. However, to date, there are few relevant studies and the metabolic pathways underlying growth limitation due to alkali tolerance are not fully understood.

Oat is a cereal crop with high economic value worldwide. Oat grains contain several health-promoting compounds, including minerals, proteins, and β -glucan, with lipid-lowering and antihypertensive effects in humans. In addition, research has demonstrated that oats are tolerant to salt and alkali stress conditions: some oat genotypes can grow under 200 mmol.L^{-1} salt stress ($NaCl:Na_2SO_4 = 1:1$) and tolerate soil $pH > 9.0$. Therefore, oats could be used to improve salt–alkali soil [23]. There is an increasing understanding of the importance of oats in improving salt–alkali soil; however, the metabolites that help increase salt and alkali tolerance remain unclear.

Widely targeted metabolomic analysis, which is based on multiple reaction monitoring (MRM) and combines the advantages of non-targeted metabolomics and targeted metabolomics [24], is a new approach and has been used in plant metabolic analyses, including analyses of *ziziphus jujuba* mill and red longan pericarp [25,26]. Widely targeted metabolomic analysis has been proven to be a very sensitive and accurate approach to the measurement of targeted metabolites.

The adverse effects of abiotic stress on plants vary at different development stages. In our previous study, under alkali stress, more severe membrane lipid peroxidation was observed at the heading stage than at the vegetative growth stage [27]. Further,

the chlorophyll content of oats decreased sharply at the booting stage compared to the vegetative growth period [23]. However, there remains a lack of understanding of the metabolic processes underlying the responses of plants to alkalinity during the reproductive growth period, particularly in the booting and heading stages.

To fill this gap, this study aimed to identify the differentially expressed metabolites (DEMs) of oat leaves under two stress conditions. The following hypotheses were tested: for oat leaves, (1) there are significant differences in metabolite profiles between salt and alkali stresses. Alkalinity inhibits crop growth more severely than salinity by modulating the expression of these metabolites. (2) There are significant changes in the contents of several metabolites under the two stress conditions, resulting in improved salt and alkali tolerance.

2. Materials and Methods

2.1. Plant Materials and Treatment Conditions

This experiment was carried out in a greenhouse at the Inner Mongolia Agricultural University in Hohhot, China, from 2019 to 2020.

The salt-alkali tolerant oat genotype OA1414-2 was used in this experiment. OA1414-2 seeds were obtained from the Ottawa Research and Development Center of Agriculture and Agri-Food Canada in Ottawa, ON, Canada. The average day/night temperature was kept at 15–25/9–15 °C, respectively, with a mean photoperiod of 14 h.

Twenty-five seeds were planted in a 25 cm tall plastic pot with 7.5 kg sand. The plants were thinned to 20 plants per plot at the two-leaf stage. The diameter of each pot was 22 cm. 500 mL of 1/2 Hoagland solution was added to each pot every third day. At the three-leaf stage, three treatments were conducted: (a) control, (b) salt stress (120 mmol.L⁻¹ NaCl:Na₂SO₄ = 1:1, 3170 us.cm⁻¹, pH 7.58), (c) alkali stress (40 mmol.L⁻¹ Na₂CO₃:NaHCO₃ = 1:1, 1279 us.cm⁻¹, pH 10.16). Under the salt stress condition, 500 mL of salt solution was added on the first day, followed by another 500 mL of salt solution two days later. Under the alkali stress condition, 500 mL of alkali solution was added on the first day, followed by another 500 mL of alkali solution two days later. The control condition received only water. Leaves were obtained at the booting stage. For each treatment, six replications were performed; each replication was represented by one pot.

2.2. Transcriptome Sequencing and Analyses

For each treatment, RNA was extracted from 0.1 g of leaves using an RNA extraction kit (Tiangen, Beijing, China). A Qubit 2.0 fluorimeter was used to determine the RNA concentration. An Agilent 2100 Bioanalyzer system (Agilent, G2939A, Santa Clara, CA, USA) was used to inspect the RNA integrity.

Magnetic oligo (dT) beads were used to enrich the mRNA and construct complementary DNA libraries; mRNA was decomposed into short fragments with fragmentation buffer, and the short fragments were used as a template for reverse transcription into first-strand cDNA with random hexamers. Then, dNTPs (dUTP, dATP, dGTP, dCTP), DNA polymerase I, and buffer were added to synthesize second-strand cDNA. AMPure XP beads were used to purify the cDNA fragments. Then, end-repair was performed, poly(A) was added, and the fragments were connected to the Illumina sequencing adapters. The ligation products were selected by AMPure XP beads, and then PCR amplification was performed.

The cDNA libraries were established and sequenced on a Novoseq 6000 platform, with a read length of 150 bp. To obtain clean reads, the adapter sequences, sequences with more than 10% poly-N, and low-quality reads (sequences with >10% ambiguous nucleotides; low-quality base numbers (Q ≤ 20) accounting for more than 50% of the sequence) were removed from the raw data. The clean reads were then mapped to the oat genome with HISAT tools (version 2.1.0). Fragments per kilobase per million mapped reads (FPKM) was used to calculate gene expression. Differentially expressed genes (DEGs) for alkali stress (AS) vs. control (CK) and salt stress (SS) vs. control (CK) were identified by DESeq software, according to specific criteria (FDR (false discover rate) < 0.05 and |log₂Fold Change| ≥ 1). Gene function was annotated based on the following databases: NR, <ftp://ftp.ncbi.nlm.nih.gov/bla>

st/db/FASTA/nr.gz; Swissprot, ftp://ftp.uniprot.org/pub/databases/uniprot/current_release/knowledgebase/complete/uniprot_sprot.fasta.gz; Pfam, <http://pfam.xfam.org/>; Tremble, ftp://ftp.uniprot.org/pub/databases/uniprot/current_release/knowledgebase/complete/uniprot_trembl.fasta.gz; KOG, <ftp://ftp.ncbi.nih.gov/pub/COG/KOG/kyva>; GO, <http://geneontology.org/docs/download-ontology/>, accessed on 14 April 2023. Enrichment analysis of GO functions and KEGG pathways was then performed for the DEGs.

2.3. Metabolite Profiling

Leaves (0.5 g) in each treatment were freeze-dried in a vacuum (Scientz-100F) for 72 h and then ground using a mixer mill (MM 400, Retsch) at 30 HZ for 1.5 min. Then, 100 mg of the powder was dissolved in 0.6 mL of 70% aqueous methanol, and the mixture was placed in a fridge (4 °C) overnight. The mixture was later centrifuged at $10,000\times g$ for 10 min. The supernatant was filtered by a micro-pore filter membrane (0.22 μ m pore size) and detected by Ultra Performance Liquid Chromatography-Tandem Mass Spectrometry (UPLC-MS/MS). A Shim-pack UFLC SHIMADZU CBM30A (China) UPLC system was used in this study. The UPLC conditions were as follows: chromatographic column, Waters ACQUITY UPLC HSS T3 C18 1.8 μ m, 2.1 mm \times 100 mm; mobile phase solvent A, 0.04% acetic acid in water; mobile phase solvent B, 0.04% acetic acid in acetonitrile; gradient program, 5% solvent B at 0 min, a linear gradient to 95% solvent B at 10 min, and 95% solvent B maintained for 1 min; the composition of solvent B decreased to 5% at 11.1 min and was maintained for 2.9 min; flow rate, 0.35 mL/min; column temperature, 40 °C; injection volume, 4 μ L.

To evaluate the repeatability of the analytical process, one quality control (QC) sample was inserted alongside each of the 10 detected samples.

Tandem mass spectrometry (Applied Biosystems 4500 QTRAP, Foster, CA, USA) was used in this study. The operation parameters for the electrospray ionization (ESI) source were as follows: source temperature, 550 °C; ion spray voltage (IS), 5500 V; curtain gas (CUR), 30 psi; collision gas (CAD), high. QQQ scans were carried out by multiple reaction monitoring (MRM) [24]. Qualitative analysis of metabolites was performed by comparing the retention time, accurate precursor ions, and product ions with the self-built database MWDB (Metware Biotechnology Co., Ltd., Wuhan, China) and public databases. In the MRM mode [24] of QQQ mass spectrometry, quantitative analysis of metabolites was carried out. The precursor ions of the target substance were filtered by quadrupole, and the ions corresponding to other molecular weights were eliminated to remove interference. The mass spectrum peaks of metabolites were integrated and corrected by MultiaQuant, and the relative metabolite levels were determined by chromatographic peak area.

Fold change ≥ 2 or ≤ 0.5 and variable importance in projection (VIP) ≥ 1 were selected as the criteria to screen DEMs. Principal component analysis (PCA) was carried out to identify the reliability and differences in the metabolic data of the samples under the three treatments using R software 3.5.0. Volcano plots were constructed using R software 3.5.0.

2.4. RT-qPCR Analysis

The total RNA of the oat leaves under the three treatments was extracted using an RNAPrep Pure Plant Kit (TIANGEN, CAT. DP432) and reverse-transcribed into first-strand cDNA using a HiScript 1st Strand cDNA Synthesis Kit (JizhenBio, CAT. AORT-0060, Shanghai, China). Real-time PCR was carried out with a Bio-Rad CFX96 Manager Real-Time PCR system. The reaction mixtures included about 10 ng of cDNA sample, 50 nmol of primers, 5 μ L of $2\times$ SYBR Green Master Mix reagent (JizhenBio, CAT. Q151-02), and water; the volume of each reaction solution was 10 μ L. The thermal cycle conditions were as follows: 95 °C for 5 min, 40 cycles of 95 °C for 10 s and 60 °C for 30 s. The qRT-PCR primers are shown in Supplementary Table S1. The *actin* gene was used as the internal control gene. The relative mRNA expression level was calculated as follows: $2^{(a-b)}$, where a is the actin Ct value of the reference gene and b is the Ct value of the target gene [28].

2.5. Chlorophyll Fluorescence Analysis

The chlorophyll fluorescence of oat leaves was determined between 10:00 and 11:00 a.m. using a portable fluorometer (PAM-2100, Walz, Nuremberg, Bavarian, Germany). Before detection, the adaxial side of the leaves was acclimated to darkness for 30 min.

The following chlorophyll fluorescence parameters were recorded: maximal fluorescence level in the dark-adapted state (F_m), minimal fluorescence level in the dark-adapted state (F_o), coefficient of photochemical quenching (qP), maximum photosystem II photochemical efficiency (F_v/F_m), non-photochemical dissipation of absorbed energy (NPQ), photosynthetic electron transport rate (ETR), and actual efficiency of photosystem II ($\Phi PSII$) (calculated according to the following formula: $\Phi PSII = (F_m' - F_s)/F_m'$ [29]).

2.6. Sodium (Na^+), Potassium (K^+), and Calcium (Ca^{2+}) Levels

The sodium (Na^+), potassium (K^+), and calcium (Ca^{2+}) levels were measured according to Rula Sa (2014) [30]. The oat leaves were dried at 105°C in an oven for 15 min and then further dried at 80 °C for two days. The samples were milled to powder; 300 mg of each powder sample was placed in 25 mL of HCl solution (1 mol.L⁻¹) and then filtered using filter paper. The levels of Na^+ and K^+ were measured by flame photometry. Then, 500 mg powder samples were placed in 20 mL of $HNO_3:HClO_4$ (4:1 v/v) solution and boiled using an electricity plate overnight. The levels of Ca^{2+} were determined using an atomic absorption spectrophotometer.

2.7. Statistical Analysis

One-way analysis of variance was performed using SPSS 26.0. $p < 0.05$ was regarded as a statistically significant difference. R software (3.5.0) was used to determine the relationships between the transcriptome and the metabolome data.

3. Results

3.1. Analysis of Transcriptomic Data

To identify the DEGs for CK vs. salinity and CK vs. alkalinity, the transcriptomic data of the oat leaves was compared across the control, salt stress, and alkali stress conditions. In the CK, salinity, and alkalinity treatments, 81,622,663, 87,254,424, and 80,621,720 raw reads were obtained and filtered, respectively, resulting in 80,011,770, 85,394,939, and 79,034,108 high-quality clean reads, respectively (Supplementary Table S2). The average number of reads was >70%, and the unique mapping rates ranged from 78.96% to 85.29%. FPKM > 1 was used as the threshold to determine gene expression. An FDR < 0.05 and fold-change ≥ 2 or ≤ 0.05 were used to select differentially expressed genes (DEGs).

Under alkalinity, 32,784 DEGs were identified (Supplementary Table S3), among which, 15,457 genes were downregulated, and 17,327 genes were upregulated. For these DEGs, the GO categories included biological processes, cellular components, and molecular function (Supplementary Figure S1). Photosynthesis was the most represented GO subcategory within the biological processes category, whereas chloroplast thylakoid membrane was the most represented GO subcategory within the cellular components category. DEGs were significantly enriched in various KEGG pathways, including metabolic pathways, biosynthesis of secondary metabolites, biosynthesis of amino acids, photosynthesis, porphyrin, and chlorophyll metabolism (Supplementary Figure S2).

Under salinity, 9123 DEGs were identified, among which, 4255 genes were downregulated, and 4868 genes were upregulated (Supplementary Table S4). For these DEGs, GO analysis indicated that several metabolic, biological, and cellular processes occurred under salt stress. Photosynthesis and cellular amino acid biosynthetic processes were enriched GO subcategories within the biological processes category, whereas intrinsic/integral components of the plasma membrane, photosystem, and photosystem II were enriched GO subcategories within the cellular components category. Anion transmembrane transporter activity was the most enriched GO subcategory within the molecular function category (Supplementary Figure S3). KEGG enrichment analysis of the DEGs revealed that several

DEGs in the salinity vs. CK comparison were involved in metabolic pathways, the biosynthesis of secondary metabolites, arginine metabolism, and proline metabolism. Chlorophyll was uniquely enriched in the alkalinity vs. CK comparison (Supplementary Figure S4).

Figure 1 indicates that salt and alkali stress conditions both affect genes related to photosynthesis. In this study, eight photosynthetic genes, encoding oxygen-evolving enhancer protein 1, oxygen-evolving enhancer protein 2, PsbP-like protein 1 (involved in the stability of PSII complexes), cytochrome b6-f complex iron–sulphur subunit, plastocyanin, ferredoxin–NADP(H) reductase (involved in electron transfer), ATP synthase subunit gamma, and ATP synthase subunit b (related to ATP production) were downregulated under alkali stress. However, these genes were not downregulated under salt stress significantly (Figure 1). Further, the chlorophyll fluorescence indices were calculated and analysed. Compared to the control condition, FO and NPQ were increased by 15.18% and 9.44% under salt stress and by 25.00% and 32.78% under alkali stress, respectively; these increases were higher under alkali stress than under salt stress. The Fv/Fm, ΦPSII, and qP values in oat leaves decreased under the two stress conditions; lower Fv/Fm, ΦPSII, and qP values were observed under alkali stress than under salt stress (Figure 2).

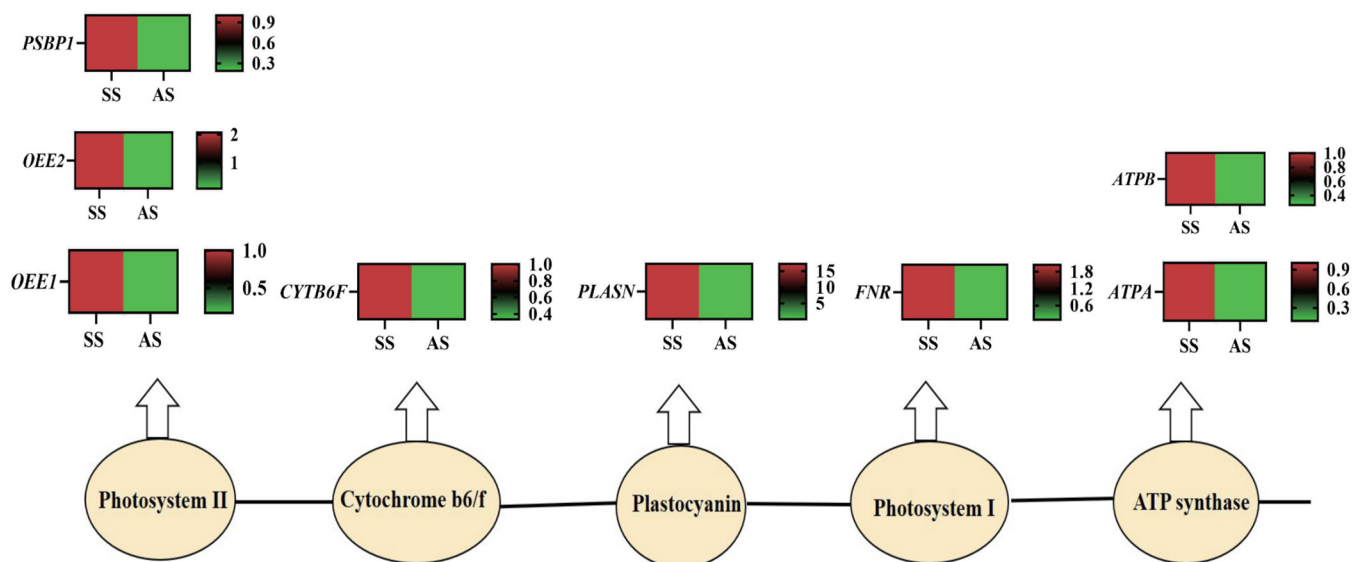


Figure 1. The differentially expressed genes (DEGs) related to photosynthesis at AS vs. CK and SS vs. CK. CK, control; AS, alkali stress ($40 \text{ mmol.L}^{-1} \text{ Na}_2\text{CO}_3:\text{NaHCO}_3 = 1:1$), SS, salt stress ($120 \text{ mmol.L}^{-1} \text{ NaCl}:\text{Na}_2\text{O}_4 = 1:1$). *OEE1*, Oxygen-evolving enhancer protein 1; *OEE2*, Oxygen-evolving enhancer protein 2; *PSBP1*, PsbP-like protein 1; *PETC*, Cytochrome b6-f complex iron–sulphur subunit; *PETE*, Plastocyanin; *LFNR*, Ferredoxin–NADP reductase; *ATP3*, ATP synthase subunit gamma; *ATPsynB*, ATP synthase subunit b.

Some genes related to chlorophyll synthesis, such as *CHLH*, *chlB*, *HEMD*, *PPO*, and one gene (*VLN3*) related to growth, were downregulated under alkali stress but did not significantly change under salt stress. Two genes involved in the biosynthesis of superoxide dismutase were upregulated under two stresses (Supplementary Table S5).

3.2. Analysis of Metabolic Data

The changes in the metabolites in the SS vs. CK and AS vs. CK conditions were detected based on MS/MS and UPLC.

To monitor the repeatability of metabolite extraction and detection, a QC sample was analysed. The total ion current (TIC) curves for the metabolites of the nine samples were highly overlapped, indicating stable signals (Figure 3).

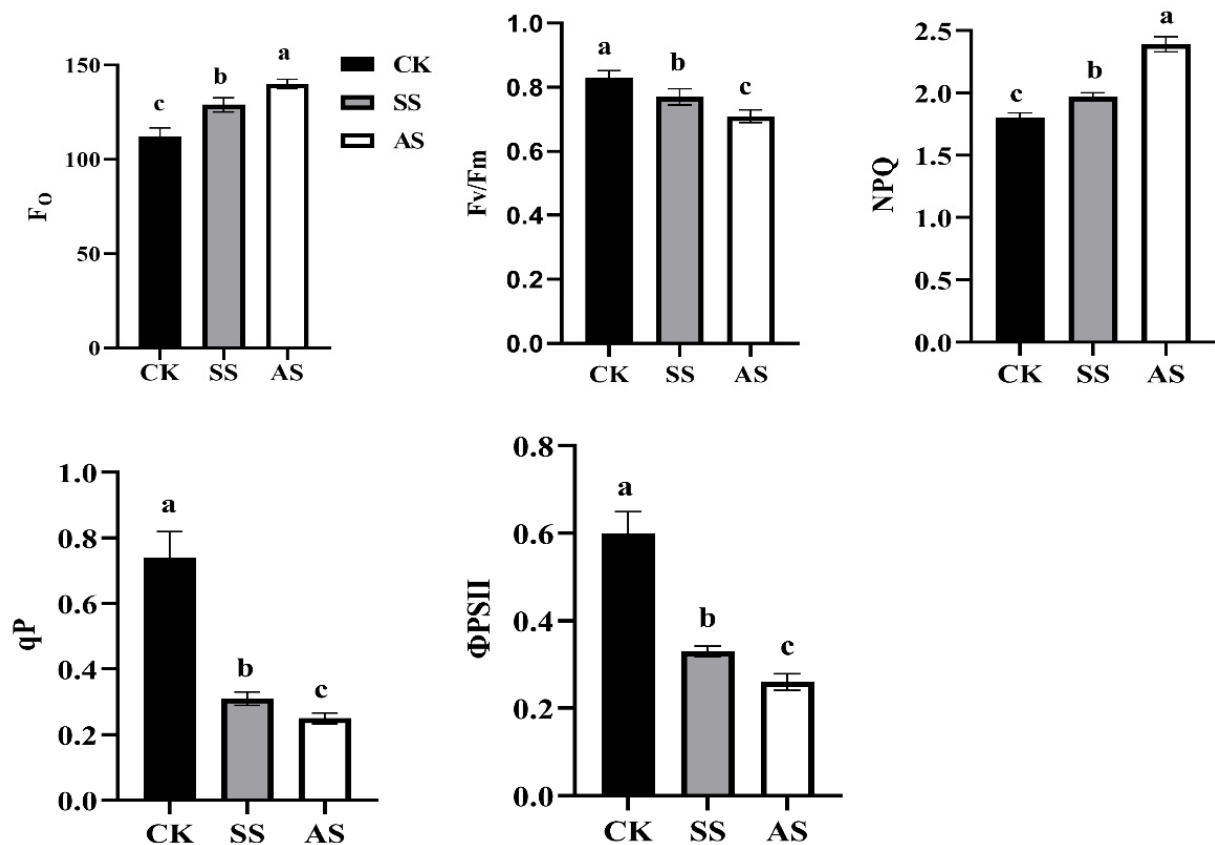
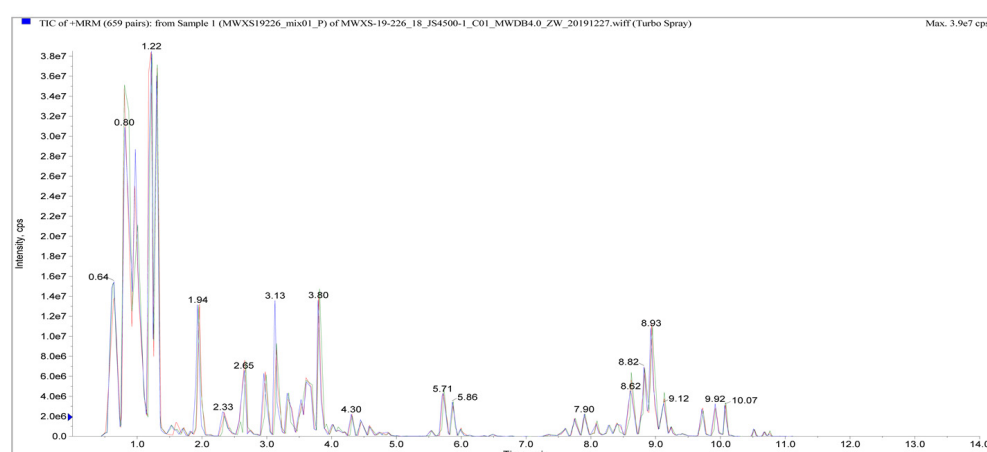


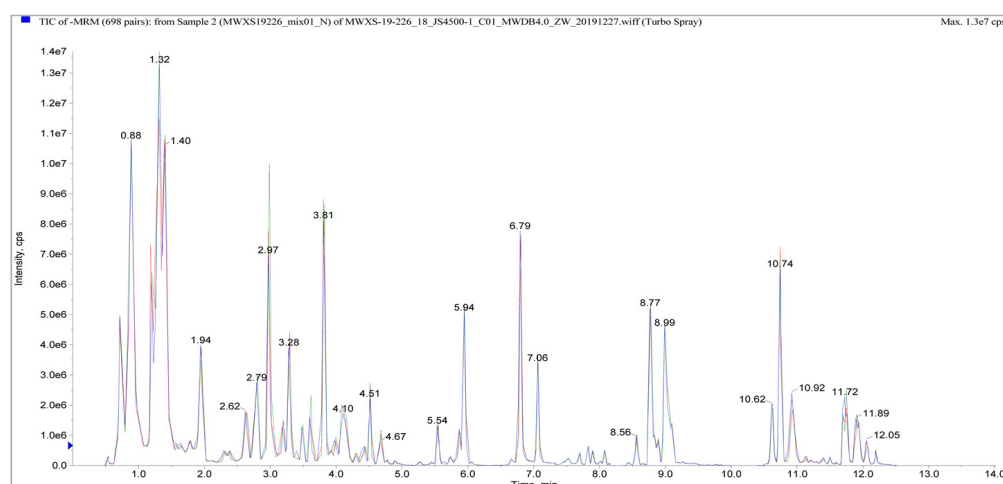
Figure 2. Effects of salt and alkali stresses on chlorophyll fluorescence parameters of oat leaves. Varied letters: significant differences at the 0.05 level. CK, control; AS, alkali stress ($40 \text{ mmol.L}^{-1} \text{ Na}_2\text{CO}_3\text{:NaHCO}_3 = 1\text{:}1$), salt stress ($120 \text{ mmol.L}^{-1} \text{ NaCl:NH}_4\text{SO}_4 = 1\text{:}1$).

The differentially accumulated metabolites (DAMs) were selected based on the following criteria: $\text{VIP} \geq 1.0$ and fold change ≥ 2 or ≤ 0.5 . Based on the metabolite quantification, a hierarchical heatmap clustering analysis of oat leaves under the three treatments was performed. Biological replicates were clustered together, suggesting that the metabolome data were of high quality. The metabolic data under salt stress were clearly separated from those from alkali stress. The PCA results indicated that the salinity, alkalinity, and CK treatments were clearly separated in the $\text{PC1} \times \text{PC2}$ score plot (Figure 4).

In total, there were 213 DAMs in the alkalinity vs. CK comparison (Supplementary Table S6, Figure 5), including 37 amino acids and derivatives (17.3%), 36 phenolic acids (16.9%), 19 nucleotides and derivatives (8.9%), 13 flavonoids (6.1%), 9 lignans and coumarins (4.2%), 22 alkaloids (10.3%), 24 organic acids (11.2%), 27 lipids (12.6%), and 26 others (12.2%). Compared with the control condition, 232 measured metabolites were significantly changed under the salinity condition (Supplementary Table S7, Figure 5), including 35 amino acids and derivatives (15.0%), 48 phenolic acids (20.6%), 18 nucleotides and derivatives (7.7%), 23 flavonoids (9.9%), 11 lignans and coumarins (4.7%), 23 alkaloids (9.9%), 1 terpenoid (0.4%), 19 organic acids (8.1%), 22 lipids (9.4%), and 32 others (13.7%). Compared to the control condition, 142 upregulated metabolites and 71 downregulated metabolites were observed under alkalinity, whereas there were 117 upregulated metabolites and 115 downregulated metabolites under salinity (Figure 5).



(A)



(B)

Figure 3. The TIC curves (A), positive-ion mode (B), negative-ion mode.

Three DAMs, including cinnamic acid and scopoline (which are related to antioxidant), decreased by 59.82% and 82.58% under alkali stress, respectively, but did not significantly change under salt stress. L-ascorbic acid (also involved in antioxidant) decreased under the two stress conditions. Protocatechuic acid (related to chlorophyll synthesis) decreased under the two stress conditions. O-coumaric acid, which inhibits plant growth, only increased under the alkalinity condition. One gene involved in o-coumaric acid synthesis was significantly upregulated under the two stress conditions; these increases were greater in the alkalinity condition, as compared to the salinity condition (Tables 1 and 2).

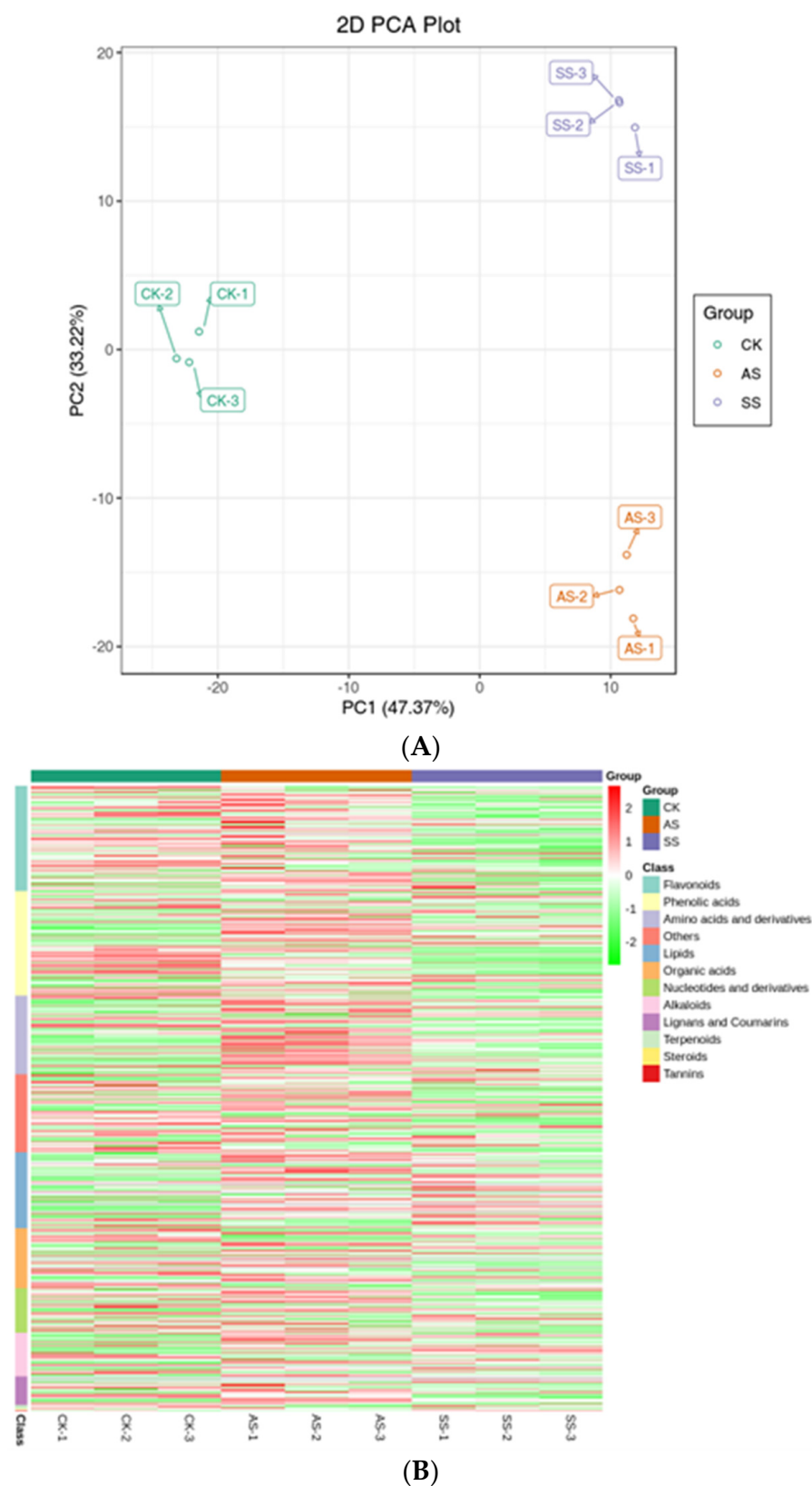


Figure 4. (A) Principal component analysis based on FPKM data; (B) The cluster heat map of differentially accumulated metabolites (DAMs) in oat leaves under control (CK), salt (SS) and alkali (AS) conditions. CK, control; AS, alkali stress ($40 \text{ mmol.L}^{-1} \text{ Na}_2\text{CO}_3\text{:NaHCO}_3 = 1\text{:}1$), SS, salt stress ($120 \text{ mmol.L}^{-1} \text{ NaCl:Na}_2\text{O}_4 = 1\text{:}1$).

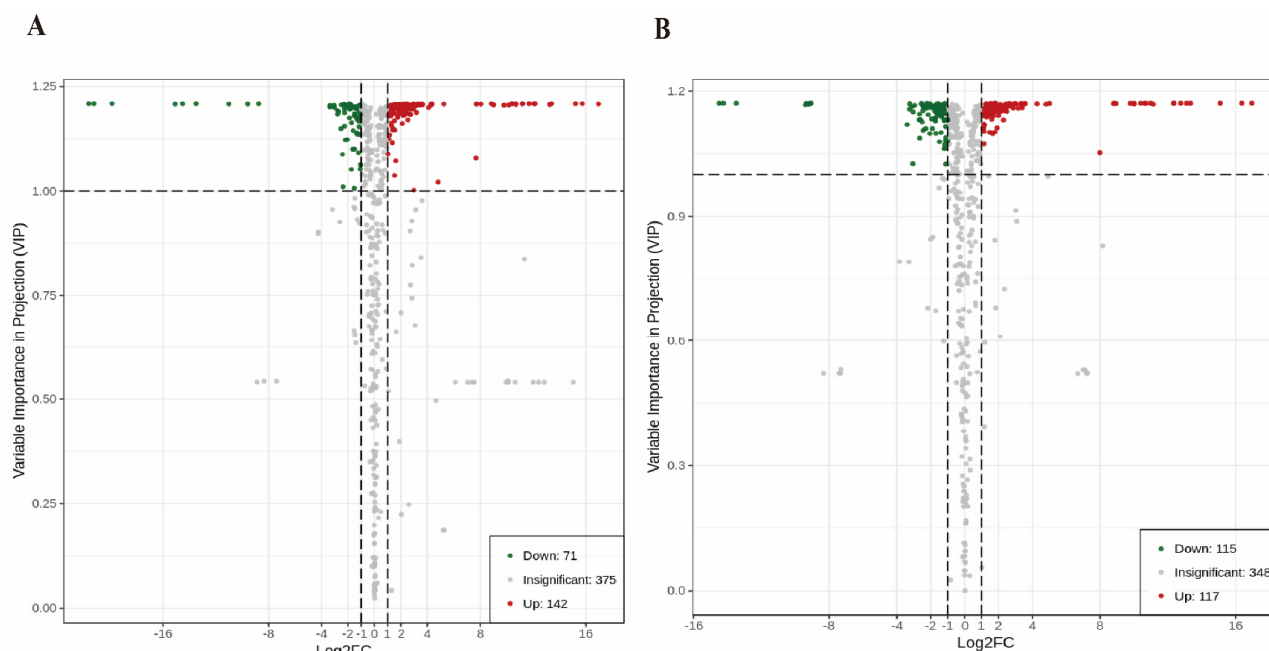


Figure 5. The Volcano plots for differentially accumulated metabolites (DAMs) at (A) AS vs. CK, (B) SS vs. CK. CK, control; AS, alkali stress ($40 \text{ mmol.L}^{-1} \text{ Na}_2\text{CO}_3\text{:NaHCO}_3 = 1\text{:}1$), salt stress ($120 \text{ mmol.L}^{-1} \text{ NaCl:Na}_2\text{SO}_4 = 1\text{:}1$).

Table 1. Some differentially expressed metabolites in oat leaves at AS vs. CK, and SS vs. CK.

ID	Function	Metabolite	Class	Response Ratio		VIP		Regulated	
				AS/CK	SS/CK	AS/CK	SS/CK	AS/CK	SS/CK
mws2213	Antioxidation	Cinnamic acid	Phenolic acids	0.40	1	1.14	-	down	No
mws1077		Scopolin	Lignans and Coumarins	0.17	1	1.15	-	down	No
Hmfn00531		L-ascorbic acid	Vitamin/others	0.46	0.41	1.21	1.16	down	down
mws0281		Citric acid	Organic acid	2.09	2.4	1.20	1.17	up	up
pme2024		Serotonin	Alkaloid	8.76	5.72	1.21	1.16	up	up
mws0263		Pyroglutamic acid	Amino acids(derivatives)	893.00	1	1.21	-	up	No
mws0282		L-tryptophan	Amino acids (derivatives)	4.87	3.26	1.21	1.17	up	up
mws0260		Arginine	Amino acids(derivatives)	9.03	4.87	1.09	1.13	up	up
pme0008		L-Citrulline	Amino acids(derivatives)	3.83	2.21	1.19	1.10	up	up
mws0014		Ferulic acid	Phenolic acid	2.50	2.46	1.19	1.14	up	up
pma6561		caffeic acid	Phenolic acid	2.42	3.23	1.20	1.26	up	up
mws0183	Chlorophyll accumulation	Protocatechuic acid	Flavanols	0.00009	0.00009	1.21	1.17	down	down
mws0275		Malic acid	Organic acid	2.98	1	1.21	-	up	No
pmb3142		Salicylic acid	Phenolic acid	126,582	84,066	1.21	1.17	up	up
pme3154		Mevalonic acid	Organic acid	54,302	10,372	1.21	1.17	Up	Up
pme1439	Growth	O-coumaric acid	Phenolic acid	2.37	1	1.18	-	up	No
mws0884	Inorganic ion regulation	Cyclic AMP	Amino acids(derivatives)	5.36	4.59	1.21	1.17	up	up
pme0006	Osmoregulation	Proline	Amino acids(derivatives)	12.1	10.65	1.21	1.17	up	up
pme2268		Trigonelline	Alkaloid	0.41	1	1.16	-	No	Down
mws0191		Betaine	Alkaloid	2.82	4.14	1.17	1.56	up	up
pmb0069	Unknown function	Benzamide	Others	206.87	456.62	1.21	1.17	up	up
mws0491		Phenethylamine	Others	212.01	446.58	1.21	1.17	up	up
mws1433		N-Feruloyltyramine	Alkaloid	1156.76	1592.89	1.21	1.17	up	up
pmb0629		Chrysoeriol	Flavonoid	3320.44	2262.04	1.21	1.17	up	up
pmb0629		6-C-hexoside	Flavonoid	3320.44	2262.04	1.21	1.17	up	up
pmb0629		1,3-O-Di-p-Coumaroyl glycerol	Phenolic acid	38,091.85	128,392.59	1.21	1.17	up	up
pmb001318	Unknown function	1,3-O-Di-p-Coumaroyl glycerol	Phenolic acid	38,091.85	128,392.59	1.21	1.17	up	up
mws1715		Cordycepin	Nucleotides(derivatives)	1356.00	1352.74	1.21	1.17	up	up

No: No significant change. CK, control; AS, alkali stress ($40 \text{ mmol.L}^{-1} \text{ Na}_2\text{CO}_3\text{:NaHCO}_3 = 1\text{:}1$), salt stress ($120 \text{ mmol.L}^{-1} \text{ NaCl:Na}_2\text{SO}_4 = 1\text{:}1$).

Table 2. The detailed information on DEGs involved in the synthesis of o-coumaric acid, serotonin, caffeic acid, citric acid, Proline, Betaine, Salicylic acid, Malic acid, L-tryptophan.

Function	Gene ID	Gene Name	Description	Fold Change		Log ₂ Fold Change		Regulated	
				SS/CK	AS/CK	SS/CK	AS/CK	SS/CK	AS/CK
O-coumaric acid synthesis	TRINITY_DN35234_c0_g1_i2.path1	CA4H	Trans-cinnamate 4-monooxygenase	2.040	40.203	1.028	5.329	up	up
Serotonin synthesis	TRINITY_DN28969_c2_g1_i1.path1	AADC	Aromatic-L-amino-acid decarboxylase	4.003	36.063	2.001	5.172	up	up
Caffeic acid	TRINITY_DN35234_c0_g1_i2.path1	CA4H	Trans-cinnamate 4-monooxygenase	2.040	40.203	1.028	5.329	up	up
	TRINITY_DN49630_c0_g1_i2.path2	C3H	p-coumarate 3-hydroxylase	0.747	0.426	−0.421	−1.231	No significant	down
Citric acid	TRINITY_DN2130_c0_g1_i1.path1	CS	Citrate synthase	2.874	32.258	1.523	5.012	up	up
Proline	TRINITY_DN22005_c0_g1_i2.path3	PIP	Proline iminopeptidase	2.046	8.934	1.033	3.159	up	up
	TRINITY_DN17408_c0_g1_i3.path1	P5CS	Delta-1-pyrroline-5-carboxylate synthase	3.563	40.663	1.833	5.346	up	up
	TRINITY_DN1782_c0_g1_i2.path1	P5CDH	Delta-1-pyrroline-5-carboxylate dehydrogenase	2.362	10.674	1.240	3.416	up	up
Betaine	TRINITY_DN33834_c0_g1_i1.path2	BADH	Betaine aldehyde dehydrogenase	2.138	9.135	1.096	3.191	up	up
Salicylic acid	TRINITY_DN5328_c0_g1_i4.path1	EDS	Enhanced disease susceptibility	2.029	3.640	1.021	1.864	up	up
	TRINITY_DN28752_c0_g1_i1.path2	PBL	avrPphB Susceptible	3.201	2.809	1.679	1.490	up	up
Malic acid	TRINITY_DN12835_c0_g1_i1.path1	MLS	Malate synthase	48.034	1137.412	5.586	10.152	up	up
	TRINITY_DN4496_c0_g1_i2.path1	FUM	Fumarase	1.945	14.678	0.96	3.876	No significant	up
L-tryptophan.	TRINITY_DN7542_c0_g1_i2.path1	TSA	Tryptophan synthase alpha chain	1.414	3.577	0.5	1.839	No significant	up
	TRINITY_DN13657_c0_g1_i2.path2	TRPB	Tryptophan synthase beta chain	0.97	3.287	−0.044	1.717	No significant	up

CA4H, Trans-cinnamate 4-monooxygenase; AADC, Aromatic-L-amino-acid decarboxylase; C3H, p-coumarate 3-hydroxylase; CS, Citrate synthase; PIP, Proline iminopeptidase; P5CS, Delta-1-pyrroline-5-carboxylate synthase; P5CDH, Delta-1-pyrroline-5-carboxylate dehydrogenase; BADH, Betaine aldehyde dehydrogenase; EDS, Enhanced disease susceptibility; PBL, avrPphB Susceptible; MLS, malate synthase; FUM, fumaric acidase; TSA, tryptophan synthase alpha chain-like; TRPB, tryptophan synthase beta chain 2; CK, control; AS, alkali stress (40 mmol.L^{−1} Na₂CO₃:NaHCO₃ = 1:1), salt stress(120 mmol.L^{−1} NaCl:Na₂O₄) = 1:1.

Several DAMs involved in ROS elimination, including citric acid, serotonin, L-citrulline, ferulic acid, and caffeic acid, were increased under the two stress conditions. Oat leaves accumulated greater levels of pyroglutamic acid, serotonin, and L-citrulline under alkali stress than under salt stress. Compared to the control condition, pyroglutamic acid increased 893.0-fold in the alkalinity condition, whereas it did not change significantly in the salinity condition. One gene that participates in serotonin biosynthesis was upregulated 36.06-fold in the alkalinity condition and increased fourfold in the salinity condition; the high expression level of this gene plays a crucial role in stimulating serotonin under salt stress. Two genes related to caffeic acid synthesis were changed under the two stress conditions. The expression level of Trans-cinnamate 4-monooxygenase (which is related to caffeic acid synthesis) increased under the two stress conditions. The citrate synthase gene, which is involved in citric acid synthesis, increased under the two stress conditions (Tables 1 and 2).

Several DAMs involved in osmoregulation, including proline, betaine, and arginine, were increased under the two stress conditions. Greater levels of proline and arginine were observed in the alkalinity condition compared to the salinity condition. Higher expression levels of three genes that take part in proline synthesis were observed in the alkalinity condition as compared to the salinity condition; this can stimulate proline accumulation. The expression level of one gene related to betaine synthesis was increased under the two stress conditions (Tables 1 and 2).

Several DAMs involved in chlorophyll synthesis, including mevalonic acid and salicylic acid, were increased under the two stress conditions. Mevalonic acid and salicylic acid

were increased 54,302.22- and 126,582.22-fold under alkali stress compared to the control condition, whereas the levels of mevalonic acid and salicylic acid increased 10,372.29- and 84,065.55-fold under salt stress. Malic acid, which is related to chlorophyll synthesis, was only increased under alkali stress. Two genes involved in salicylic acid biosynthesis were upregulated under the two stress conditions. The expression level of the fumarase gene, which is related to malic acid synthesis, only increased significantly under alkali stress. The expression level of the malate synthase gene, which is involved in malic acid synthesis, increased 1137.4-fold under alkali stress and 48.034-fold under salt stress, as compared to the control condition; high expression levels of these two genes under alkali stress play a crucial role in stimulating malic acid synthesis and accumulation.

In this study, salinity and alkalinity facilitated the accumulation of Na^+ and decreased the levels of K^+ and Ca^{2+} (Supplementary Figure S5), whereas the cyclic AMP levels (related to inorganic ion metabolism) were increased under the two stress conditions. Moreover, L-tryptophan levels, related to hormone metabolism, increased under the two stress conditions; the expression levels of two genes related to tryptophan synthesis were also increased in the alkalinity condition but did not change significantly in the salinity condition (Tables 1 and 2).

There were 148 changed metabolites in both the alkalinity vs. CK comparison and the salinity vs. CK comparison. Only 65 DAMs were found in the alkalinity vs. CK comparison, including o-coumaric acid; 84 DAMs were identified in the salinity vs. CK comparison, including trigonelline (Supplementary Figure S6).

To validate the transcriptome results, 16 DEGs were selected and the expression levels of these DEGs were analysed by qPCR. The gene expression patterns in qPCR were similar to the transcriptome results (Figure 6).

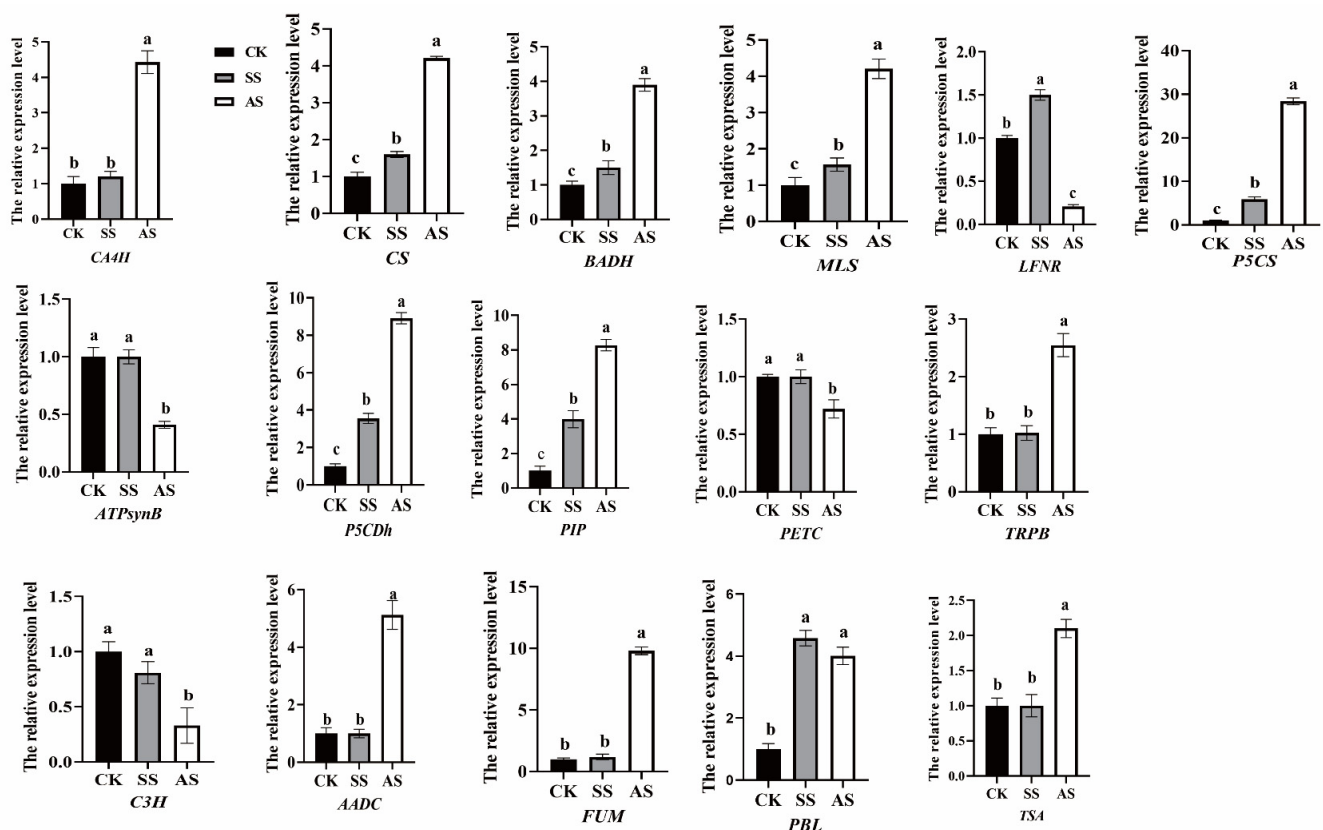


Figure 6. The quantitative RT-PCR analysis of some genes. The values are the mean \pm SE of three independent biological replicates normalized against the reference gene Actin. *CA4H*, Trans-cinnamate 4-monooxygenase; *CS*, Citrate synthase; *BADH*, Betaine aldehyde dehydrogenase; *MLS*, malate synthase; *LFNR*, Ferredoxin NADP reductase; *PIP*, Proline iminopeptidase; *ATPsynB*, ATP

synthase subunit b; *P5CHh*, Delta-1-pyrroline-5-carboxylate dehydrogenase; *P5CS*, Delta-1-pyrroline-5-carboxylate synthase; *PETC*, Cytochrome b6-f complex iron-sulphur subunit; *C3H*, p-coumarate 3-hydroxylase; *AADC*, Aromatic-L-amino-acid decarboxylase; *FUM*, fumarase; *PBL*, avrPphB Susceptible; *TRPB*, tryptophan synthase beta chain; *TSA*, tryptophan synthase alpha chain. CK, control; AS, alkali stress (40 mmol.L⁻¹ Na₂CO₃:NaHCO₃ = 1:1); SS, salt stress (120 mmol.L⁻¹ NaCl:Na₂O₄) = 1:1. Different letters are significantly different at 0.05 probability level.

The levels of benzamide, phenethylamine, N-feruloyltyramine, chrysoeriol 6-C-hexoside, 1,3-O-di-p-coumaroyl glycerol, cordycepin, and 1-o-p-coumaroylglycerol increased by 206.87, 212.01, 1156.76, 3320.44, 38,091.85, 1356.00, and 38,091.85 under alkali stress compared to the control condition. The accumulation of these metabolites under alkali stress has not been observed in other plant species (Table 1).

4. Discussion

4.1. Genes Related to Growth Inhibition, Chlorophyll Content Decrease and Antioxidation Due to the Two Stress Conditions

The expression levels of eight genes related to photosynthesis, and some chlorophyll synthesis genes, including *PPO*, *HEMD*, *chlB*, *CHLH*, decreased in alkalinity. However, these genes were not downregulated in salinity significantly, which may be one reason why alkalinity inhibits chlorophyll accumulation and photosynthetic rate more severely than salinity.

Plant actin plays an important role in cell growth. Bundling of actin filaments is likely mediated by actin-bundling proteins, such as villins. Hannie [31] has proved that double mutant plants in which *VILLIN2* and *VILLIN3* transcripts are truncated, have twisted leaves, stems, indicating an important role for villin in the regulation of directional organ growth. In this study, the expression of *VILLIN3* decreased under alkali stress; however, it did not change significantly under salt stress, which may be one reason why alkalinity inhibits plant growth more severely than salinity.

SOD dismutates O₂^{•-} to O₂ and H₂O₂. In this study, the expression of superoxide dismutase (SOD) synthesis genes, including *MnSOD*, *CuZnSOD*, increased under salt and alkali stress, which would contribute to the elimination of reactive oxygen species (ROS).

4.2. Metabolites Related to Growth Inhibition and Chlorophyll Content Decrease Due to the Two Stress Conditions

Alkalinity inhibited crop production more severely than salinity. This is the first report to demonstrate comprehensive differences in metabolic profiling between salt and alkali stress conditions at the booting stage. One important question is: which metabolic pathways inhibited by alkali stress further adversely affects oat growth? To answer this question, we identified the differentially expressed metabolites in alkalinity compared to the control.

The role of metabolites in inhibiting plant growth under alkali stress has not been elucidated. In the photosynthetic electron transport chain, electrons transfer from reduced ferredoxin to oxygen instead of to NADP, and ROS are produced. Thus, the photosynthetic organs are vulnerable to ROS, especially in stressful environments, such as drought and salt stress conditions [32]. Our results revealed that alkali stress triggered a decrease in the levels of cinnamic acid, L-ascorbic acid (LAA), and scopoline. Previous studies have proved that cinnamic acid stimulates antioxidant enzyme activities and reduces lipid peroxidation to some extent, together with the finding that the application of cis-cinnamic acid stimulates both cell division and cell expansion in arabidopsis leaves [33]. Scopoline in leaves is thought to scavenge reactive oxygen species (ROS). Döll et al. (2018) [34] have reported that scopoline levels were triggered by abiotic stress such as cold or high sucrose, and the accumulation of scopoline contributes to ROS scavenging under stress conditions. In this study, the levels of cis-cinnamic acid and scopoline decreased under alkali stress but did not change significantly under salt stress, which may be one reason why alkalinity

causes more severe oxidative stress and growth inhibition than salinity. It has been reported that H_2O_2 can be scavenged by LAA [32]. Thus, in our study, the decrease in LAA levels in leaves was observed under alkali and salt stress conditions, which may contribute to the accumulation of H_2O_2 and facilitate oxidative stress.

Our previous study demonstrated that alkalinity induces the appearance of yellow leaves, decreases the chlorophyll content, and thereby reduces yield production. However, the detailed molecular mechanism for the decrease in chlorophyll content in alkalinity remains unclear. Xuan et al. (2018) [35] have proven that exogenous protocatechuic acid could improve the chlorophyll content, and thereby facilitate the photosynthetic rate improvement of rice. Our results showed a significant reduction in protocatechuic acid under alkali stress, which contributes to the decrease in chlorophyll content.

O-coumaric acid, a vital phenolic acid, has been considered to be a plant growth inhibitor. Hossain et al. (2005) [36] have proven that exogenous p-coumaric acid inhibits cell elongation by increasing the content of cell wall-bound phenolic compounds, which could decrease cell wall extensibility [36]. In this study, the enhanced accumulation of o-coumaric acid was observed under alkali stress, but not under salt stress, suggesting that the more severe growth inhibition due to alkalinity than salinity may be related to the increase in o-coumaric acid levels due to alkalinity. In addition, we proved the expression level of genes (*CA4H*) involved in O-coumaric acid synthesis also increased under alkali stress, the increasing level of *CA4H* was higher in alkalinity than in salinity.

It has been reported that trigonelline plays a role in osmoregulation to prevent water loss within plant cells [37]. In this study, the levels of trigonelline, an alkaloid, decreased under salt stress but did not change significantly under alkali stress. The reduction in trigonelline levels in oat leaves would make the water loss more severe under salt stress.

4.3. Metabolic Pathways Related to the Improvement of Salt and Alkali Tolerance

4.3.1. Metabolites Related to the Improvement of the Chlorophyll Content under Salt and Alkali Stress Conditions

Inhibitory effects of alkali conditions on chlorophyll accumulation have been reported, but the role of metabolites in improving the chlorophyll content has not been completely explored. Mevalonic acid, an important organic acid, plays important roles in the synthesis of functional plastidic isoprenoids, such as carotenoids and chlorophylls, which contribute to plastid development [38]. Indeed, there have been reports that mevalonic acid is related to chlorophyll synthesis. For instance, Nagata et al. (2002) [38] proved that the chlorophyll formation ability was limited in *Arabidopsis cla1-1* mutants (a null mutant of the first-step enzyme in the MEP pathway). The application of mevalonic acid to *Arabidopsis cla1-1* mutants led to substantial recovery of chlorophyll fluorescence and plastid development. In this study, salt and alkali stress conditions led to an increase in mevalonic acid levels in oat leaves. Furthermore, alkalinity led to 5.4-fold higher mevalonic acid levels than salinity, suggesting that alkali-induced accumulation of mevalonic acid was beneficial for oats to increase their chlorophyll content.

Guo et al. (2017a) [39] reported that malic acid, an organic acid, contributes to increasing photosynthetic capacity. Supplementation with malic acid effectively enhances the chlorophyll content in *Lilium* [40]. Results from our data indicated that malic acid levels increased in alkalinity but did not change significantly in salinity; similar malic acid changes have also been noted in maize under alkali stress conditions [41]. This result indicated that alkalinity-induced inhibition of chlorophyll accumulation could be alleviated by malic acid. Our results also proved that two genes involved in malic acid synthesis were upregulated in alkalinity, which would facilitate the malic acid accumulation.

To assess the effects of salt and alkali stress conditions on the PSII reaction centre, a key part of photosynthesis, we tested the chlorophyll fluorescence parameters of oat leaves. Our data showed that the two stress conditions induced a decrease in F_v/F_m and $\Phi PSII$, and alkalinity led to more decrease in the values of F_v/F_m and $\Phi PSII$ than salinity, suggesting that excess alkaline salts indicate photochemical reaction damage,

and that the inhibition of electron transport occurs at the PSII acceptor side, between the primary acceptor plastoquinone (QA) and the secondary acceptor plastoquinone (QB), disturbing the PSII reaction centre more severely. Furthermore, our previous reports found that oxygen evolution complex (OEC) protein, a key part of the photosynthetic apparatus, was downregulated under salt and alkali stress conditions, thereby decreasing the photosynthetic rate (P_n) [42].

Salicylic acid, a vital phenolic acid, has been regarded as a regulatory signal mediating plant responses to abiotic stress conditions. Nie et al. (2018) [43] found that supplementation with salicylic acid alleviated chlorophyll degradation and growth inhibition of cucumber due to alkalinity and protected the structural stability of OEC as well as the PSII reaction centre by enhancing the expression levels of *Cab* (LHC protein gene), *psbA* (D1 protein gene), and *psbB* (D2 protein gene).

In this study, we got similar results: salicylic acid levels in oat leaves increased by 126,582-fold under alkali stress and by 84,065-fold under salt stress, and there were more salicylic acid levels in alkalinity than in salinity, which might help enhance the chlorophyll content and protect the structural stability of OEC and the PSII reaction centre under alkali stress. The higher expression levels of two genes (*EDS*, *PBL*) in alkalinity (or salinity) compared to the control may be the reason for the accumulation of salicylic acid led by two stresses.

4.3.2. Metabolites Related to the Elimination of ROS under Salt and Alkali Stress Conditions

Abiotic stress-induced ROS production is an important phenomenon leading to plant growth inhibition. Our previous reports indicated that alkali stress causes higher levels of ROS in oat leaves than salt stress [20]. The initial defence against oxidative damage is provided by antioxidant enzymes, such as SOD and POD. Tahjib-Ul-Arif et al. (2021) [44] showed that exogenous application of citric acid markedly increased the activity of CAT and SOD under salt stress in cotton. Ferulic acid and caffeic acid, two phenolic acids, have been regarded as candidates for increasing plant tolerance to abiotic stress by increasing antioxidant activity. Thus, in this study, the accumulation of citric acid, ferulic acid, and caffeic acid due to salinity and alkalinity contributed to ROS scavenging [45,46]. The gene (*CA4H*) for biosynthesis of caffeic acid synthesis and the gene (*CS*) for biosynthesis of citric acid have the higher expression levels under two stresses compared to the control, which would facilitate the accumulation of caffeic acid and citric acid.

Serotonin is an important alkaloid required not only for ROS elimination but also for delaying senescence in leaves. Gupta et al., 2017 [47] found that increased production of serotonin was observed in salt-tolerant cultivars, whereas the sensitive cultivars failed to produce serotonin under salt stress, which suggests the positive role of serotonin in combating salt stress. In the present study, serotonin was identified in oat leaves and increased in response to the two stress conditions, and alkalinity induced higher serotonin accumulation than salinity, which may contribute to ROS scavenging and improve alkali tolerance. One gene (*AADC*) was upregulated under two stresses, which may contribute to the serotonin accumulation.

In this study, the accumulation of several amino acids was the important response of oats to exposure to alkali or salt stress conditions. According to a previous study, supplementation with pyroglutamic acid has been proven to increase the antioxidant defences and photosynthesis rate under water stress [48]. However, the role of pyroglutamic acid in regulating alkali tolerance has not been elucidated. Our study showed that oat leaves accumulated 893-fold higher pyroglutamic acid under alkali stress than the control, supporting a positive role for pyroglutamic acid in alkali resistance. This is not in agreement with a previous report that showed that alkali stress caused a decreased level of pyroglutamic acid in sunflower. The discrepancies may be due to the differences in plant species [49]. Although salt stress is severe, pyroglutamic acid levels did not change significantly in salinity, suggesting that the mechanisms of pyroglutamic acid response to the two stress conditions were different. It has been proved that in plants, L-pyroglutamic acid can be

converted into glutamic acid and that glutamic acid acts as a precursor in proline biosynthesis [48]. However, in soybean, exogenous glutamic acid did not improve the proline level. Jiménez-Arias hypothesized that the conversion of pyroglutamic acid to glutamic acid and finally to proline only occurs under stress conditions [50]. In this study, pyroglutamic acid and proline were both upregulated under alkali stress; however, glutamic acid decreased in alkalinity, which did not support this hypothesis.

In this study, increased levels of amino acids, such as proline, L-tryptophan, arginine, and L-citrulline, were observed in oat leaves under salt and alkali stress conditions. Previous study shows that alkali stress increases proline and L-tryptophan contents in canola [51]. L-tryptophan is an important amino acid required not only for ROS scavenging but also for the positive modification of plant physiological processes. In addition, L-tryptophan is an active precursor of auxin (IAA) [52,53]. Zahir et al. (2010) [54] found that supplementation with L-tryptophan facilitated IAA production and nutrient uptake and increased the grain yield of mung bean under salt stress [54]. Our previous reports proved that alkali stress causes IAA accumulation in oats [23]. In this study, the improvement of L-tryptophan due to alkalinity may be the reason for the observed increase in IAA levels. Our results confirmed the increased expression of genes (*TSA*, *TRPB*) involved in L-tryptophan synthesis under two stresses, and the increasing levels were higher in alkalinity than in salinity, which may be the immediate cause for the higher accumulation of L-tryptophan under alkali stress than under salt stress.

In addition, it has been proven that exogenous arginine could alleviate the oxidative damage due to water stress in tomato [55]. L-citrulline is an efficient hydroxyl radical scavenger [56]. Proline not only serves as a vital osmoregulation substance but also plays an important role in active oxygen scavenging. In this study, alkali stress led to high levels of proline, L-tryptophan, L-citrulline, and arginine than salt stress, which may play a role in alleviating the severe oxidative damage induced by alkalinity.

Under alkali, salt stresses, arginine contents increased by 8.03, 3.87-fold, and proline contents increased by 11.1, 9.65-fold. In addition, arginine is a precursor of proline, and the enhancement of arginine may be the reason for the observed increase in proline. The genes (*PIP*, *P5C5*, *P5CDH*) related to proline synthesis were upregulated under two stresses, which may be the reason for proline accumulation.

4.3.3. Metabolites Related to Inorganic Ion Regulation

In plants, cyclic AMP, which is regarded as a second messenger, functions in regulating responses to varied abiotic stress conditions. Previous study has proved that cyclic AMP leads to the deactivation of voltage-independent channels, decreasing unidirectional Na^+ influx and increasing salt tolerance [57]. Cyclic AMP functions in increasing cytosolic free Ca^{2+} levels through targeting membrane cyclic nucleotide-gated channels (CNGCs) [58]. In this study, salt and alkali stress conditions led to an increase in Na^+ levels and a decrease in K^+ and Ca^{2+} levels, which were toxic to oats. In addition, our results show the upregulation of cyclic AMP in oat leaves led by salt and alkali stress conditions, which may help inhibit Na^+ influx and increase Ca^{2+} levels. In addition, Paradiso et al. (2020) [58] found that the failure in cyclic AMP elevation during heat stress caused a high accumulation of reactive oxygen species, the cyclic AMP is related to antioxidation. The accumulation of Cyclic AMP led by alkalinity and salinity may be related to ROS elimination.

Jayakannan et al. (2013) [59] proved that salicylic acid increases the H^+ -ATPase, reduces salinity-induced membrane depolarization, limits K^+ leakage, and improves the K^+ level. Salicylic acid could also regulate the KOR channel (GORK), proton (H^+) pump activity, affect salt overly sensitive 1 (SOS1) expression, and reduce Na^+ under salt stress [60]. Therefore, in this study, the increase in salicylic acid contents in oat leaves led by salt and alkali stress conditions contributes to maintaining ion balance, decreasing the adverse effects of stress conditions on photosynthetic organs.

Our results also reveal that some metabolites, such as N-feruloyltyramine, chrysoeriol 6-C-hexoside, 1,3-o-di-p-coumaroyl glycerol, cordycepin, 1-o-p-coumaroylglycerol, benza-

mide, and phenethylamine accumulated under alkali stress; this phenomenon has not been observed in other plant species. The functions of these metabolites in alkali tolerance remain unclear and need to be further studied.

5. Conclusions

The increase in o-coumaric acid levels, the decreased accumulation of cis-cinnamic acid, scopolin, and protocatechuic acid were observed under alkali stress, which may inhibit oat growth and chlorophyll synthesis. The levels of cis-cinnamic acid, scopolin, and o-coumaric acid did not change under salt stress, which explains the phenomenon that alkalinity inhibited oat growth more severely than salinity. The enhancement of levels of citric acid, serotonin, pyroglutamic acid, L-citrulline, ferulic acid, and caffeic acid, mevalonic acid, salicylic acid, cyclic AMP were observed under two stresses, which may help improve salt and alkali tolerance. Eight photosynthetic genes and some chlorophyll synthesis genes decreased under alkali stress and did not change under salt stress, which could be the reason for the lower photosynthetic rate in alkalinity than in salinity. Seven metabolites were identified to be responding to alkalinity, their functions in alkali tolerance remain unclear, and need to study further.

Supplementary Materials: The following supporting information can be downloaded at: <https://www.mdpi.com/article/10.3390/agronomy13061441/s1>, Supplementary Figure S1: GO analysis of differentially expressed genes in oat leaves at AS vs. CK. CK, control; AS, alkali stress (40 mmol.L⁻¹ Na₂CO₃:NaHCO₃ = 1:1); Supplementary Figure S2: KEGG analysis of differentially expressed genes in oat leaves at AS vs. CK. CK, control; AS, alkali stress (40 mmol.L⁻¹ Na₂CO₃:NaHCO₃ = 1:1); Supplementary Figure S3: GO analysis of differentially expressed genes in oat leaves at SS vs. CK. CK, control; SS, salt stress (120 mmol.L⁻¹ NaCl:Na₂SO₄) = 1:1; Supplementary Figure S4: KEGG analysis of differentially expressed genes in oat leaves at SS vs. CK. CK, control; SS, salt stress (120 mmol.L⁻¹ NaCl:Na₂SO₄) = 1:1; Supplementary Figure S5: Effects of salt and alkali stress on contents of Na⁺, K⁺, Ca²⁺ in oat leaves. Varied letters: significant differences at the 0.05 level. CK, control; AS, alkali stress (40 mmol.L⁻¹ Na₂CO₃:NaHCO₃ = 1:1), salt stress(120 mmol.L⁻¹ NaCl:Na₂SO₄) = 1:1; Supplementary Figure S6: Venn diagrams of DEGs among different treatments (CK, AS, SS) CK, control; AS, alkali stress (40 mmol.L⁻¹ Na₂CO₃:NaHCO₃ = 1:1), salt stress(120 mmol.L⁻¹ NaCl:Na₂SO₄) = 1:1; Supplementary Table S1: The primers used for RT-qPCR; Supplementary Table S2: The quality control of transcriptional data; Supplementary Table S3: Differentially expressed genes in oat leaves at alkalinity vs. CK. CK, control; Alkalinity, alkali stress (40 mmol.L⁻¹ Na₂CO₃:NaHCO₃ = 1:1); Supplementary Table S4: Differentially expressed genes in oat leaves at salinity vs. CK. CK, control; salinity, salt stress (120 mmol.L⁻¹ NaCl:Na₂SO₄) = 1:1; Supplementary Table S5: Some differentially expressed genes in oat leaves at AS vs. CK, and SS vs. CK. CK, control condition; SS, salt stress (120 mmol.L⁻¹ NaCl:Na₂SO₄) = 1:1; AS, alkali stress (40 mmol.L⁻¹ Na₂CO₃:NaHCO₃ = 1:1); Supplementary Table S6: The differentially expressed metabolites in oat leaves at AS vs. CK. CK, control; AS, alkali stress (40 mmol.L⁻¹ Na₂CO₃:NaHCO₃ = 1:1); Supplementary Table S7: The differentially expressed metabolites in oat leaves at SS vs. CK. CK, control; salt stress (120 mmol.L⁻¹ NaCl:Na₂SO₄) = 1:1.

Author Contributions: J.B. designed this experiment. J.B. conducted the experiment and wrote this paper. P.L., F.L. participated in the experiment. L.L. and Q.Y. helped process data and revise this paper. All authors have read and agreed to the published version of the manuscript.

Funding: This work was supported by the double first-class construction funds (RK2200001420), the scientific research support funds for the introduction of high-level talents in 2021 (DC2200000575), Inner Mongolia Science and Technology Project (2022YFXZ0031), National Natural Science Foundation of China (31901459), and Science and Technology Major Project of Ordos (2022EEDSKJZDZX011).

Data Availability Statement: All data are contained in manuscript.

Acknowledgments: We thank Weikai Yan (Eastern Cereal and Oilseed Research Centre, Agriculture and Agri-Food Canada) for giving us the oat seeds.

Conflicts of Interest: The authors declare no conflict of interest.

References

- Cheng, M.C.; Liao, P.M.; Kuo, W.W.; Lin, T.P. The Arabidopsis ETHYLENE RESPONSE FACTOR1 regulates abiotic stress-responsive gene expression by binding to different cis-acting elements in response to different stress signals. *Plant Physiol.* **2013**, *162*, 1566–1582. [\[CrossRef\]](#) [\[PubMed\]](#)
- Liu, X.; Chai, J.; Zhang, Y.; Zhang, C.; Lei, Y.; Li, Q.; Yao, T. Halotolerant rhizobacteria mitigate the effects of salinity stress on maize growth by secreting exopolysaccharides. *Environ. Exp. Bot.* **2022**, *204*, 105098. [\[CrossRef\]](#)
- Zhang, W.; Wei, J.; Guo, L.; Fang, H.; Liu, X.; Liang, K.; Niu, W.; Liu, F.; Siddique, K.H.M. Effects of Two Biochar Types on Mitigating Drought and Salt Stress in Tomato Seedlings. *Agronomy* **2023**, *13*, 1039. [\[CrossRef\]](#)
- Li, H.; Tang, X.; Yang, X.; Zhang, H. Comprehensive transcriptome and metabolome profiling reveal metabolic mechanisms of *Nitraria sibirica* Pall. to salt stress. *Sci. Rep.* **2021**, *11*, 12878. [\[CrossRef\]](#) [\[PubMed\]](#)
- Niron, H.; Barlas, N.; Salih, B.; Türet, M. Comparative Transcriptome, Metabolome, and Ionome Analysis of Two Contrasting Common Bean Genotypes in Saline Conditions. *Front. Plant Sci.* **2020**, *11*, 599501. [\[CrossRef\]](#)
- Song, T.; Xu, H.; Sun, N.; Jiang, L.; Tian, P.; Yong, Y.; Yang, W.; Cai, H.; Cui, G. Metabolomic Analysis of Alfalfa (*Medicago sativa* L.) Root-Symbiotic Rhizobia Responses under Alkali Stress. *Front. Plant Sci.* **2017**, *8*, 1208. [\[CrossRef\]](#)
- Bai, J.; Yan, W.; Wang, Y.; Yin, Q.; Liu, J.; Wight, C.; Ma, B. Screening Oat Genotypes for Tolerance to Salinity and Alkalinity. *Front. Plant Sci.* **2018**, *9*, 1302. [\[CrossRef\]](#)
- Deinlein, U.; Stephan, A.B.; Horie, T.; Luo, W.; Xu, G.; Schroeder, J.I. Plant salt-tolerance mechanisms. *Trends Plant Sci.* **2014**, *19*, 371–379. [\[CrossRef\]](#)
- Yu, Z.; Duan, X.; Luo, L.; Dai, S.; Ding, Z.; Xia, G. How Plant Hormones Mediate Salt Stress Responses. *Trends Plant Sci.* **2020**, *25*, 1117–1130. [\[CrossRef\]](#)
- Zhu, J.K. Plant salt tolerance. *Trends Plant Sci.* **2001**, *6*, 66–71. [\[CrossRef\]](#)
- Mushtaq, Z.; Faizan, S.; Gulzar, B. Salt stress, its impacts on plants and the strategies plants are employing against it: A review. *J. Appl. Biochem. Biotechnol.* **2020**, *8*, 81–91.
- Wen, W.; Li, K.; Alseekh, S.; Omranian, N.; Zhao, L.; Zhou, Y.; Xiao, Y.; Jin, M.; Yang, N.; Liu, H.; et al. Genetic Determinants of the Network of Primary Metabolism and Their Relationships to Plant Performance in a Maize Recombinant Inbred Line Population. *Plant Cell* **2015**, *27*, 1839–1856. [\[CrossRef\]](#)
- Kim, H.K.; Choi, Y.H.; Verpoorte, R. NMR-based plant metabolomics: Where do we stand, where do we go? *Trends Biotechnol.* **2011**, *29*, 267–275. [\[CrossRef\]](#) [\[PubMed\]](#)
- Khan, N.; Ali, S. Advances in detection of stress tolerance in plants through metabolomics approaches. *Plant Omics* **2017**, *10*, 153–163. [\[CrossRef\]](#)
- Zhang, Y.; Li, D.; Zhou, R.; Wang, X.; Dossa, K.; Wang, L.; Zhang, Y.; Yu, J.; Gong, H.; Zhang, X.; et al. Transcriptome and metabolome analyses of two contrasting sesame genotypes reveal the crucial biological pathways involved in rapid adaptive response to salt stress. *BMC Plant Biol.* **2019**, *19*, 66. [\[CrossRef\]](#)
- Wu, D.; Cui, M.; Hao, Y.; Liu, L.; Zhou, Y.; Wang, W.; Xue, A.; Chingin, K.; Luo, L. In Situ Study of Metabolic Response of *Arabidopsis thaliana* Leaves to Salt Stress by Neutral Desorption-Extractive Electrospray Ionization Mass Spectrometry. *J. Agric. Food Chem.* **2019**, *67*, 12945–12952. [\[CrossRef\]](#)
- Ma, S.; Lv, L.; Meng, C.; Zhang, C.; Li, Y. Integrative Analysis of the Metabolome and Transcriptome of *Sorghum bicolor* Reveals Dynamic Changes in Flavonoids Accumulation under Saline-Alkali Stress. *J. Agric. Food Chem.* **2020**, *68*, 14781–14789. [\[CrossRef\]](#)
- Guo, R.; Shi, L.; Yang, C.; Yan, C.; Zhong, X.; Liu, Q.; Xia, X.; Li, H. Comparison of Ionic and Metabolites Response under Alkali Stress in Old and Young Leaves of Cotton (*Gossypium hirsutum* L.) Seedlings. *Front. Plant Sci.* **2016**, *7*, 1785. [\[CrossRef\]](#)
- Song, T.; Sun, N.; Dong, L.; Cai, H. Enhanced alkali tolerance of rhizobia-inoculated alfalfa correlates with altered proteins and metabolic processes as well as decreased oxidative damage. *Plant Physiol. Biochem.* **2021**, *159*, 301–311. [\[CrossRef\]](#)
- Qin, Y.; Bai, J.; Wang, Y.; Liu, J.; Hu, Y.; Dong, Z.; Ji, L. Comparative effects of salt and alkali stress on photosynthesis and root physiology of oat at anthesis. *Arch. Biol. Sci.* **2017**, *70*, 50. [\[CrossRef\]](#)
- Jia, X.; Wang, H.; Svetla, S.; Zhu, Y.; Hu, Y.; Cheng, L.; Zhao, T.; Wang, Y. Comparative physiological responses and adaptive strategies of apple *Malus halliana* to salt, alkali and saline-alkali stress. *Sci. Hortic.* **2019**, *245*, 154–162. [\[CrossRef\]](#)
- Obata, T.; Witt, S.; Lisec, J.; Palacios-Rojas, N.; Florez-Sarasa, I.; Yousfi, S.; Araus, J.L.; Cairns, J.E.; Fernie, A.R. Metabolite Profiles of Maize Leaves in Drought, Heat, and Combined Stress Field Trials Reveal the Relationship between Metabolism and Grain Yield. *Plant Physiol.* **2015**, *169*, 2665–2683. [\[CrossRef\]](#)
- Bai, J.; Jin, K.; Qin, W.; Wang, Y.; Yin, Q. Proteomic Responses to Alkali Stress in Oats and the Alleviatory Effects of Exogenous Spermine Application. *Front. Plant Sci.* **2021**, *12*, 627129. [\[CrossRef\]](#) [\[PubMed\]](#)
- Chen, W.; Gong, L.; Guo, Z.; Wang, W.; Zhang, H.; Liu, X.; Yu, S.; Xiong, L.; Luo, J. A novel integrated method for large-scale detection, identification, and quantification of widely targeted metabolites: Application in the study of rice metabolomics. *Mol. Plant.* **2013**, *6*, 1769–1780. [\[CrossRef\]](#) [\[PubMed\]](#)
- Li, S.; Deng, B.; Tian, S.; Guo, M.; Liu, H.; Zhao, X. Metabolic and transcriptomic analyses reveal different metabolite biosynthesis profiles between leaf buds and mature leaves in *Ziziphus jujuba* mill. *Food Chem.* **2021**, *347*, 129005. [\[CrossRef\]](#) [\[PubMed\]](#)
- Yi, D.; Zhang, H.; Lai, B.; Liu, L.; Pan, X.; Ma, Z.; Wang, Y.; Xie, J.; Shi, S.; Wei, Y. Integrative Analysis of the Coloring Mechanism of Red Longan Pericarp through Metabolome and Transcriptome Analyses. *J. Agric. Food Chem.* **2021**, *69*, 1806–1815. [\[CrossRef\]](#) [\[PubMed\]](#)

27. Bai, J.-H.; Liu, J.-H.; Zhang, N.; Yang, J.-H.; Sa, R.-L.; Wu, L. Effect of Alkali Stress on Soluble Sugar, Antioxidant Enzymes and Yield of Oat. *J. Integr. Agric.* **2013**, *12*, 1441–1449. [\[CrossRef\]](#)
28. Livak, K.J.; Schmittgen, T.D. Analysis of relative gene expression data using real-time quantitative PCR and the 2[−]11 CT method. *Methods* **2001**, *25*, 402–408. [\[CrossRef\]](#)
29. Li, G.; Wan, S.; Zhou, J.; Yang, Z.; Qin, P. Leaf chlorophyll fluorescence, hyperspectral reflectance, pigments content, malondialdehyde and proline accumulation responses of castor bean (*Ricinus communis* L.) seedlings to salt stress levels. *Ind. Crops Prod.* **2010**, *31*, 13–19. [\[CrossRef\]](#)
30. Sa, R.L.; Liu, J.H.; Liu, W.; Jiao, W.H.; Bai, J.H.; Wang, Z.H. Effects of salt stress and alkali stress on the content of Na⁺, K⁺ and yield of oat seedlings. *Acta Agric. Boreali-Occident Sin.* **2014**, *23*, 50–54.
31. Hannie, S.; Kieft, H.; Emons, A.; Ketelaar, T. Arabidopsis *VILLIN2* and *VILLIN3* Are Required for the Generation of Thick Actin Filament Bundles and for Directional Organ Growth. *Plant Physiol.* **2012**, *158*, 1426–1438.
32. Davey, M.W.; Montagu, M.V.; Inzé, D.; Sanmartin, M.; Kanellis, A.; Smirnoff, N.; Benzie, I.J.J.; Strain, J.J.; Favell, D.; Fletcher, J. Plant L-ascorbic acid: Chemistry, function, metabolism, bioavailability and effects of processing. *J. Sci. Food Agric.* **2000**, *80*, 825–860. [\[CrossRef\]](#)
33. Li, Q.; Yu, B.; Gao, Y.; Dai, A.-H.; Bai, J.-G. Cinnamic acid pretreatment mitigates chilling stress of cucumber leaves through altering antioxidant enzyme activity. *J. Plant Physiol.* **2011**, *168*, 927–934. [\[CrossRef\]](#) [\[PubMed\]](#)
34. Döll, S.; Kuhlmann, M.; Rutten, T.; Mette, M.F.; Scharfenberg, S.; Petridis, A.; Berreth, D.C.; Mock, H.P. Accumulation of the coumarin scopolin under abiotic stress conditions is mediated by the Arabidopsis thaliana THO/TREX complex. *Plant J.* **2018**, *93*, 431–444. [\[CrossRef\]](#) [\[PubMed\]](#)
35. Xuan, T.D.; Khang, D.T. Effects of Exogenous Application of Protocatechuic Acid and Vanillic Acid to Chlorophylls, Phenolics and Antioxidant Enzymes of Rice (*Oryza sativa* L.) in Submergence. *Molecules* **2018**, *23*, 620. [\[CrossRef\]](#)
36. Hossain, A.K.M.Z.; Ohno, T.; Koyama, H.; Hara, T. Effect of Enhanced Calcium Supply on Aluminum Toxicity in Relation to Cell Wall Properties in the Root Apex of Two Wheat Cultivars Differing in Aluminum Resistance. *Plant Soil* **2005**, *276*, 193–204. [\[CrossRef\]](#)
37. Mohamadi, N.; Sharififar, F.; Pournamdari, M.; Ansari, M. A Review on Biosynthesis, Analytical Techniques, and Pharmacological Activities of Trigonelline as a Plant Alkaloid. *J. Diet. Suppl.* **2018**, *15*, 207–222. [\[CrossRef\]](#)
38. Nagata, N.; Suzuki, M.; Yoshida, S.; Muranaka, T. Mevalonic acid partially restores chloroplast and etioplast development in Arabidopsis lacking the non-mevalonate pathway. *Planta* **2002**, *216*, 345–350. [\[CrossRef\]](#)
39. Guo, H.; Chen, H.; Hong, C.; Jiang, D.; Zheng, B. Exogenous malic acid alleviates cadmium toxicity in *Miscanthus sacchariflorus* through enhancing photosynthetic capacity and restraining ROS accumulation. *Ecotoxicol. Environ. Saf.* **2017**, *141*, 119–128. [\[CrossRef\]](#)
40. Darandeh, N.; Hadavi, E. Effect of Pre-Harvest Foliar Application of Citric Acid and Malic Acid on Chlorophyll Content and Post-Harvest Vase Life of Liliun cv. Brunello. *Front. Plant Sci.* **2011**, *2*, 106. [\[CrossRef\]](#)
41. Guo, R.; Shi, L.; Yan, C.; Zhong, X.; Gu, F.; Liu, Q.; Xia, X.; Li, H. Ionomeric and metabolic responses to neutral salt or alkaline salt stresses in maize (*Zea mays* L.) seedlings. *BMC Plant Biol.* **2017**, *17*, 41. [\[CrossRef\]](#) [\[PubMed\]](#)
42. Bai, J.; Qin, Y.; Liu, J.; Wang, Y.; Sa, R.; Zhang, N.; Jia, R. Proteomic response of oat leaves to long-term salinity stress. *Environ. Sci. Pollut. Res. Int.* **2017**, *24*, 3387–3399. [\[CrossRef\]](#) [\[PubMed\]](#)
43. Nie, W.; Gong, B.; Chen, Y.; Wang, J.; Wei, M.; Shi, Q. Photosynthetic capacity, ion homeostasis and reactive oxygen metabolism were involved in exogenous salicylic acid increasing cucumber seedlings tolerance to alkaline stress. *Sci. Hortic.* **2018**, *235*, 413–423. [\[CrossRef\]](#)
44. Tahjib-Ul-Arif, M.; Zahan, M.I.; Karim, M.M.; Imran, S.; Hunter, C.T.; Islam, M.S.; Mia, M.A.; Hannan, M.A.; Rhaman, M.S.; Hossain, M.A.; et al. Citric Acid-Mediated Abiotic Stress Tolerance in Plants. *Int. J. Mol. Sci.* **2021**, *22*, 7235. [\[CrossRef\]](#) [\[PubMed\]](#)
45. Yildiztugay, E.; Ozfidan-Konakci, C.; Karahan, H.; Kucukoduk, M.; Turkan, I. Ferulic acid confers tolerance against excess boron by regulating ROS levels and inducing antioxidant system in wheat leaves (*Triticum aestivum*). *Environ. Exp. Bot.* **2019**, *161*, 193–202. [\[CrossRef\]](#)
46. Wan, Y.-Y.; Chen, S.-Y.; Huang, Y.-W.; Li, X.; Zhang, Y.; Wang, X.-J.; Bai, J.-G. Caffeic acid pretreatment enhances dehydration tolerance in cucumber seedlings by increasing antioxidant enzyme activity and proline and soluble sugar contents. *Sci. Hortic.* **2014**, *173*, 54–64. [\[CrossRef\]](#)
47. Gupta, P.; De, B. Metabolomics analysis of rice responses to salinity stress revealed elevation of serotonin, and gentisic acid levels in leaves of tolerant varieties. *Plant Signal. Behav.* **2017**, *12*, e1335845. [\[CrossRef\]](#)
48. Jiménez-Arias, D.; García-Machado, F.J.; Morales-Sierra, S.; Luis, J.C.; Suarez, E.; Hernández, M.; Valdés, F.; Borges, A.A. Lettuce plants treated with L-pyrogutamic acid increase yield under water deficit stress. *Environ. Exp. Bot.* **2019**, *158*, 215–222. [\[CrossRef\]](#)
49. Lu, H.; Wang, Z.; Xu, C.; Li, L.; Yang, C. Multiomics analysis provides insights into alkali stress tolerance of sunflower (*Helianthus annuus* L.). *Plant Physiol. Biochem.* **2021**, *166*, 66–77. [\[CrossRef\]](#)
50. Teixeira, W.F.; Fagan, E.B.; Soares, L.H.; Umburanas, R.C.; Reichardt, K.; Neto, D.D. Foliar and Seed Application of Amino Acids Affects the Antioxidant Metabolism of the Soybean Crop. *Front. Plant Sci.* **2017**, *8*, 327. [\[CrossRef\]](#)
51. Wang, W.; Pang, J.; Zhang, F.; Sun, L.; Yang, L.; Zhao, Y.; Yang, Y.; Wang, Y.; Siddique, K.H.M. Integrated transcriptomics and metabolomics analysis to characterize alkali stress responses in canola (*Brassica napus* L.). *Plant Physiol. Biochem.* **2021**, *166*, 605–620. [\[CrossRef\]](#) [\[PubMed\]](#)

52. Mustafa, A.; Imran, M.; Ashraf, M.; Mahmood, K. Perspectives of Using L-Tryptophan for Improving Productivity of Agricultural Crops: A Review. *Pedosphere* **2018**, *28*, 16–34. [[CrossRef](#)]
53. Khan, N.; Bano, A.; Rahman, M.A.; Rathinasabapathi, B.; Babar, M.A. UPLC-HRMS-based untargeted metabolic profiling reveals changes in chickpea (*Cicer arietinum*) metabolome following long-term drought stress. *Plant Cell Environ.* **2019**, *42*, 115–132. [[CrossRef](#)] [[PubMed](#)]
54. Zahir, Z.A.; Shah, M.K.; Naveed, M.; Akhter, M.J. Substrate-dependent auxin production by *Rhizobium phaseoli* improves the growth and yield of *Vigna radiata* L. under salt stress conditions. *J. Microbiol. Biotechnol.* **2010**, *20*, 1288–1294. [[CrossRef](#)] [[PubMed](#)]
55. Nasibi, F.; Yaghoobi, M.M.; Kalantari, K.M. Effect of exogenous arginine on alleviation of oxidative damage in tomato plant underwater stress. *J. Plant Interact.* **2011**, *6*, 291–296. [[CrossRef](#)]
56. Akashi, K.; Miyake, C.; Yokota, A. Citrulline, a novel compatible solute in drought-tolerant wild watermelon leaves, is an efficient hydroxyl radical scavenger. *FEBS Lett.* **2001**, *508*, 438–442. [[CrossRef](#)]
57. Sabetta, W.; Vannini, C.; Sgobba, A.; Marsoni, M.; Paradiso, A.; Ortolani, F.; Bracale, M.; Viggiano, L.; Blanco, E.; de Pinto, M.C. Cyclic AMP deficiency negatively affects cell growth and enhances stress-related responses in tobacco Bright Yellow-2 cells. *Plant Mol. Biol.* **2016**, *90*, 467–483. [[CrossRef](#)]
58. Paradiso, A.; Domingo, G.; Blanco, E.; Buscaglia, A.; Fortunato, S.; Marsoni, M.; Scarcia, P.; Caretto, S.; Vannini, C.; de Pinto, M.C. Cyclic AMP mediates heat stress response by the control of redox homeostasis and ubiquitin-proteasome system. *Plant Cell Environ.* **2020**, *43*, 2727–2742. [[CrossRef](#)]
59. Jayakannan, M.; Bose, J.; Babourina, O.; Rengel, Z.; Shabala, S. Salicylic acid improves salinity tolerance in *Arabidopsis* by restoring membrane potential and preventing salt-induced K⁺ loss via a GORK channel. *J. Exp. Bot.* **2013**, *64*, 2255–2268. [[CrossRef](#)]
60. Chen, H.N.; Tao, L.Y.; Shi, J.M.; Han, X.R.; Cheng, X.G. Exogenous salicylic acid signal reveals an osmotic regulatory role in priming the seed germination of *Leymus chinensis* under salt-alkali stress. *Environ. Exp. Bot.* **2021**, *188*, 104498.

Disclaimer/Publisher's Note: The statements, opinions and data contained in all publications are solely those of the individual author(s) and contributor(s) and not of MDPI and/or the editor(s). MDPI and/or the editor(s) disclaim responsibility for any injury to people or property resulting from any ideas, methods, instructions or products referred to in the content.